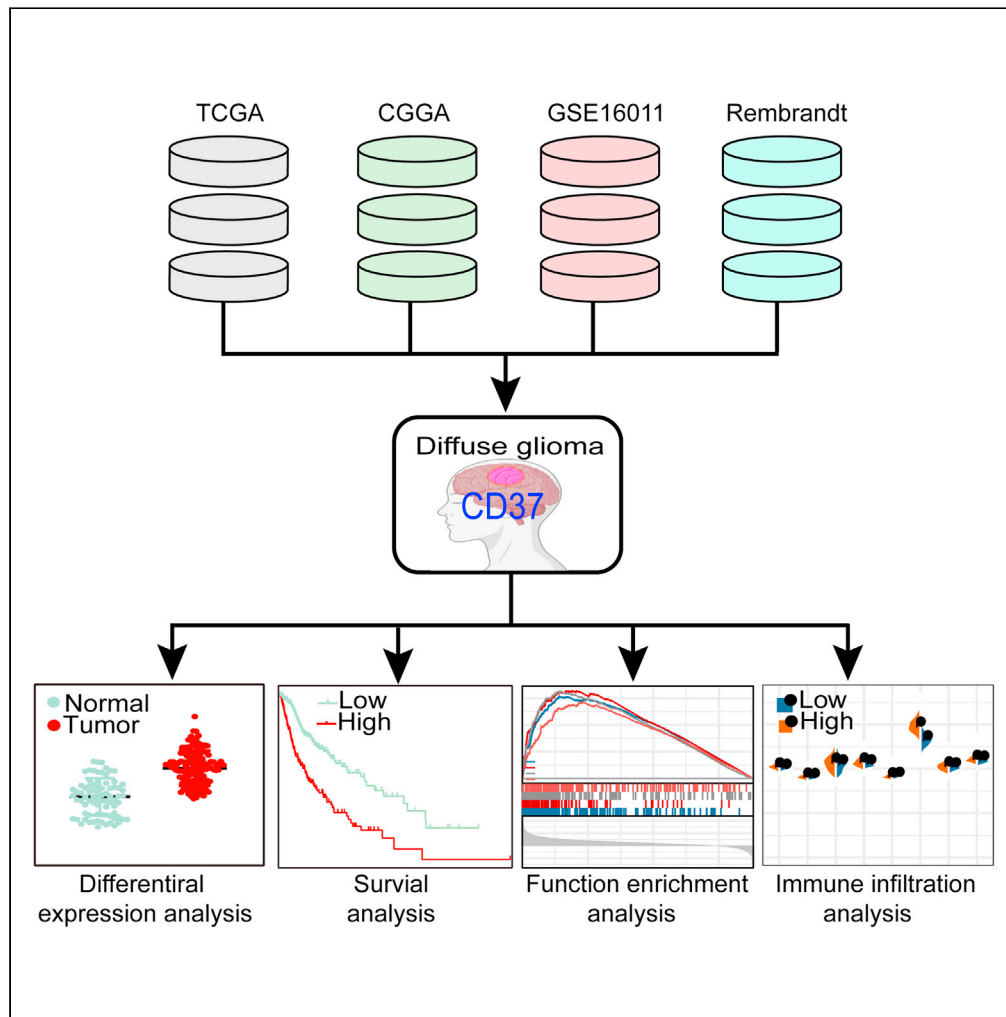# iScience

Article

The clinical features, prognostic significance, and immune heterogeneity of CD37 in diffuse gliomas

Xuejun Yan,
Quanwei Zhou,
Hecheng Zhu, ...,
Ming Zhao,
Xingjun Jiang,
Caiping Ren

rencaiping@csu.edu.cn (C.R.)
jiangxj@csu.edu.cn (X.J.)

Highlights

Diffuse gliomas with high CD37 expression exhibited a malignant phenotype

CD37 serves as an independent unfavorable prognostic factor for diffuse gliomas

CD37 remodels the immunosuppressive microenvironment of diffuse gliomas

Targeting CD37 may be a promising immunotherapeutic strategy for diffuse gliomas

iScience

Article

The clinical features, prognostic significance, and immune heterogeneity of CD37 in diffuse gliomas

Xuejun Yan,[1,4,5] Quanwei Zhou,[2,5] Hecheng Zhu,[3] Weidong Liu,[1,4] Hongjuan Xu,[1,4] Wen Yin,[2] Ming Zhao,[3] Xingjun Jiang,[2,*] and Caiping Ren[1,2,4,6,*]

SUMMARY

Diffuse glioma is the most prevalent and malignant brain tumor. The function and significance of CD37 in diffuse gliomas remain largely unknown. Here, we showed CD37 was abnormally expressed in diverse cancers, especially glioma by pan-cancer differential expression analysis. In addition, we found CD37 was upregulated in higher grade and IDH or IDH1-wildtype gliomas, which was further validated by qPCR and IHC. Survival analysis revealed CD37 served as an independent indicator for unfavorable prognosis of patients with diffuse gliomas. Functional enrichment analysis revealed CD37 was associated with immunological processes. Moreover, immune infiltration analyses suggested gliomas with high-expression CD37 had greater infiltration of M2 macrophages and neutrophils, and lower NK cell abundance. CD37 was closely correlated to immune checkpoint molecules, including CD276, CD80, CD86, and PD-L2. Our results indicated CD37 is an independent prognostic factor and plays an immunosuppressive role in diffuse gliomas. Targeting CD37 could be a promising immunotherapeutic strategy for diffuse gliomas.

INTRODUCTION

Diffuse glioma is the most common tumor of the central nervous system (CNS), accounting for more than 80% of brain malignancies (Schwartzbaum et al., 2006), and is characterized by extensive invasion toward adjacent brain tissue (Louis et al., 2016). According to the 2016 World Health Organization Classification of Tumors of the Central Nervous System, the WHO grade II and grade III astrocytic tumors, grade II and III oligodendrogliomas, the grade IV glioblastomas, and the related diffuse gliomas of childhood are all classified to diffuse gliomas (Louis et al., 2016). Diffuse gliomas exhibit a wide range of prognoses depending on the grade, from 1 to 15 years of median overall survival (Martínez-Ricarte et al., 2018). Despite multimodal treatments, including surgical resection combined with radiotherapy and/or chemotherapy, patients with glioblastoma multiforme (GBM) have a median survival of only approximately 14 months (Stupp et al., 2009; Perry et al., 2017). Although patients with grade II-III glioma have a relatively favorable prognosis, with a median survival of more than 7 years (Suzuki et al., 2015), patients frequently relapse and progress to a higher grade of diffuse glioma, leading to treatment resistance and ultimately treatment failure (Ostrom et al., 2016). Standard treatment alone has difficulty extending patient survival, therefore, new therapeutic strategies for diffuse gliomas are urgently needed. In recent years, antitumor immunotherapies, such as CAR-T cells and inhibitors of PD-1/PD-L1 (programmed death-1/programmed death ligand-1), have shown satisfactory effects in diverse malignant tumors (Yi et al., 2018). In addition, the genetic landscapes of diffuse gliomas have been extensively studied (Cancer Genome Atlas Research Network et al., 2015), which provides a new perspective for identifying molecular targets for immunotherapy in diffuse gliomas.

Diffuse gliomas are characterized by a highly immunosuppressive and heterogeneous tumor microenvironment that is considered to be a key regulator of malignant progression in primary tumors (Friebel et al., 2020; Quail and Joyce, 2017). The microenvironment consists of stromal cells and immune cells, including fibroblasts, endothelial cells, neutrophils, natural killer (NK) cells, and tumor-associated macrophages (TAMs) (Quail and Joyce, 2017). Among immune cells, macrophages account for nearly 30% of tumor mass (Graeber et al., 2002). Unlike M1 macrophages, tumor-associated macrophages (M2 macrophages)

[1]Cancer Research Institute, Department of Neurosurgery, Xiangya Hospital, Central South University, Changsha, Hunan 410008, China

[2]Department of Neurosurgery, Xiangya Hospital, Central South University, Changsha, Hunan 410008, China

[3]Changsha Kexin Cancer Hospital, Changsha, Hunan 410205, China

[4]The NHC Key Laboratory of Carcinogenesis and The Key Laboratory of Carcinogenesis and Cancer Invasion of the Chinese Ministry of Education, School of Basic Medical Science, Central South University, Changsha 410008, China

[5]These authors contributed equally

[6]Lead contact

*Correspondence: rencaiping@csu.edu.cn (C.R.), jiangxj@csu.edu.cn (X.J.)

play an immunosuppressive role by blocking T-cell proliferation and inhibiting the cytotoxic T lymphocyte response (Murray et al., 2014), contributing to the immunosuppressive microenvironment in diffuse gliomas. Studies have shown that tumor-associated macrophages reduce proinflammatory cytokines and key molecules involved in T cell co-stimulation, such as CD40, CD80, and CD86, suggesting that they have a poor response to targeted T cells in gliomas (Hussain et al., 2006). Considering the immuno-suppressive effect of M2 macrophages in promoting glioma progression, targeting M2 macrophages may be an effective way to block tumor progression. In addition, neutrophils are enriched in high-grade gliomas and serve as a robust indicator of an unfavorable prognosis (Zhang et al., 2017; Zhou et al., 2020). Recent studies have suggested that neutrophils promote tumor progression by releasing factors to enhance extracellular matrix remodeling, stimulate angiogenesis, and regulate other inflammatory cells. The factors released by neutrophils can also directly promote the proliferation and invasion of tumor cells. GBM with increased tumor-infiltrating neutrophils exhibits more aggressive tumor progression. Chemo-therapy and anti-VEGF resistance are associated with increased infiltration of neutrophils (Liang et al., 2014). These studies have shown that tumor-infiltrating lymphocytes, for example, tumor-infiltrating neu-trophils (TINs) and TAMs, can affect the efficacy and prognosis of patients treated with chemotherapy and immunotherapy, whereas many patients with glioma are refractory to current immunotherapy. This has aroused great interest in identifying crucial immunotherapeutic molecular targets to enhance the effi-cacy of immunotherapy for glioma (Reardon et al., 2014).

CD37 is a member of the tetraspanin superfamily, with a four-passage transmembrane structure, and is specifically expressed in lymphoid tissues by macrophages, neutrophils, and B cells (Meyer-Wentrup et al., 2007). Accumulating literatures indicate that the biological function of CD37 involves the migration of lymphocytes (Wee et al., 2015) and T cell proliferation (van Spriel et al., 2004). Although CD37 is ex-pressed at very low levels in T cells (Schwartz-Albiez et al., 1988), patients with high CD37 expression have poor prognosis and are suitable for CAR T-cell approaches (Pereira et al., 2015; Cooper et al., 2018). In addition, as reported in the literatures, CD37 promotes neutrophil adhesion and recruitment via the promotion of cytoskeletal function downstream of integrin-mediated adhesion (Wee et al., 2015). Clinically, CD37 represents a promising target for B- and T-cell lymphoma therapy and has recently been validated as a druggable target, with anti-CD37 monoclonal antibodies and antibody-drug conju-gates being used in clinical trials of both B- and T-cell lymphoma (Pagel et al., 2015). These findings indicate that CD37 is involved in regulating tumor-infiltrating lymphocytes. However, the role of CD37 in affecting lymphocyte immune infiltration in diffuse gliomas remains unclear.

In this work, to reveal the underlying role of CD37 across cancers, we first thoroughly explored the mRNA expression of CD37 in normal tissues and tumor tissues. Then, we comprehensively analyzed the correla-tion between the mRNA expression of CD37 and clinical features as well as prognosis in over 2000 glioma samples. Highly expressed CD37 was frequently found in glioblastoma, high-grade glioma, and IDH or IDH1 wild-type glioma and was accompanied by poor prognosis. Multiple immune infiltration analyses showed that CD37 expression was positively correlated with immune scores and stromal scores. In addi-tion, glioma patients with high expression of CD37 had a higher infiltrating abundance of M2 macrophages and neutrophils and a lower NK cell abundance. Moreover, the expression of CD37 was closely related to some immune checkpoint biomarkers, such as CD40, CD48, LGALS9, CD86, and PD-L2. These findings elucidate the crucial relationship and an underlying mechanism between CD37 expression and tumor im-mune infiltration, which provides a new immunotherapy strategy for patients with diffuse glioma.

RESULTS

CD37 is differentially expressed in normal tissues and pan-cancer tissues

We first extracted the mRNA expression data of CD37 in 31 types of normal tissues from the GTEx dataset. A significant difference in the mRNA expression level of CD37 was observed, with relatively lower expres-sion in muscle, pancreas, heart, skin, and brain tissues ($p < 0.001$, Figure 1A). Then, we further analyzed the differential expression of CD37 in 20 types of tumor tissues and corresponding normal tissues from the TCGA dataset. The findings revealed significant differences in 12 kinds of tumors compared to their corre-sponding normal tissues, with higher CD37 expression in seven types of tumor tissues, including GBM, and lower CD37 expression in five types of tumor tissues ($p < 0.05$, Figure 1B); there was no significant differ-ence between ESCA, KICH, LGG, PAAD, PRAD, STAD, THCA or UCEC tissues and the corresponding normal tissues. To compensate for the deficiency of limited normal tissue samples in the TCGA cohort, we combined the GTEx and TCGA databases to collect gene expression data from normal tissues. We
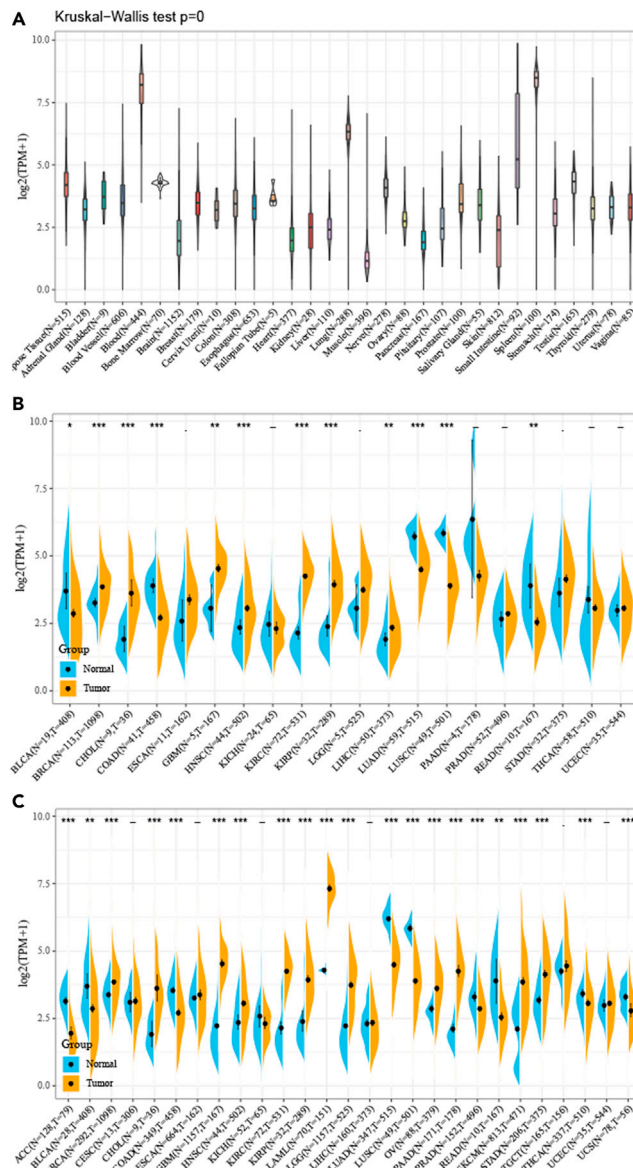
Figure 1. The expression level of CD37 in normal tissues and pan-cancer

(A) The expression level of CD37 in normal tissues.

(B) The difference of CD37 expression between tumor and normal tissues from the TCGA dataset.

(C) The difference of CD37 expression between tumor and normal tissues from an integrated dataset by combining the GTEx database with the TCGA database. ("−" means no significance, *, **, *** mean p < 0.05, p < 0.01, p < 0.001, respectively).

discovered that 21 out of 27 types of cancers had abnormally high expression of CD37, suggesting that CD37 plays an important biological role in tumor progression (p < 0.05, Figure 1C). In particular, CD37 was significantly overexpressed in 12 types of tumor tissues, such as LGG and GBM, compared to the corresponding normal tissues (p < 0.05, Figure 1C). In short, our results showed that CD37 was heterogeneously expressed in normal tissues and abnormally and highly expressed in a variety of tumors.

CD37 is associated with the malignant phenotype of diffuse gliomas

To explore the underlying significance of CD37 in diffuse gliomas, we analyzed the relationships between CD37 expression and three important clinicopathological parameters, including the WHO grade system,
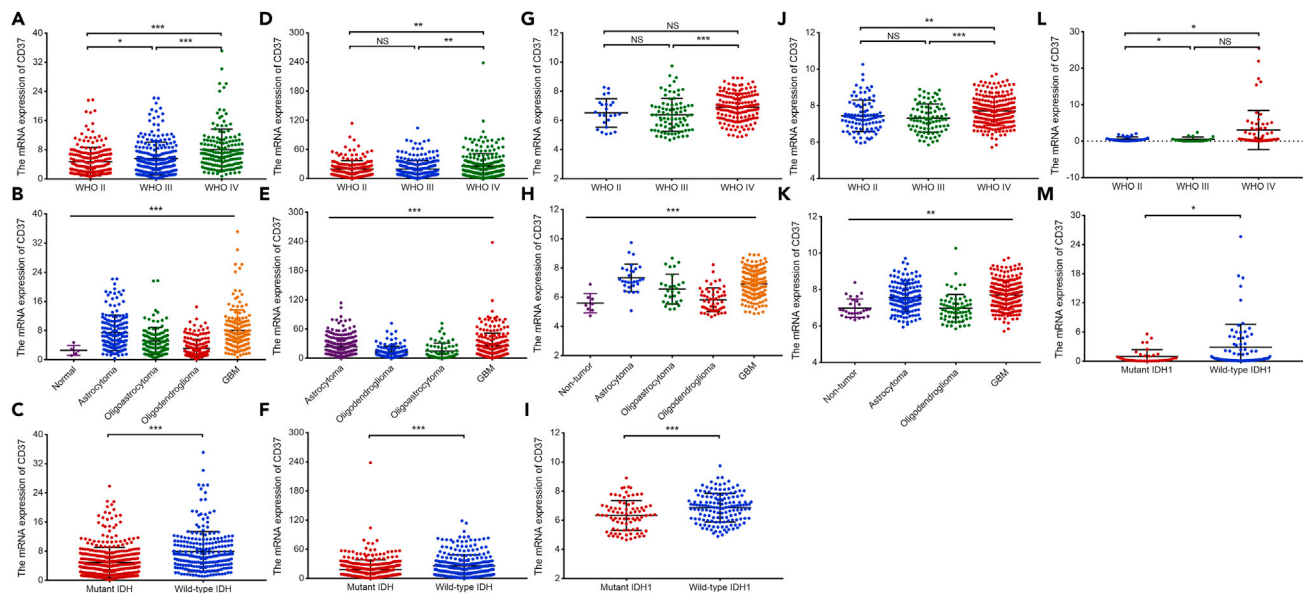
Figure 2. Correlations between CD37 expression and WHO grades, histology types, and IDH1 or IDH mutant status in the five cohorts

(A–C) Correlations between CD37 expression and WHO grade (A), histology types (B), and IDH mutant status (C) in the TCGA cohort.

(D–F) Correlations between CD37 expression and WHO grade (D), histology types (E), and IDH mutant status (F) in the CGGA cohort.

(G–I) Correlations between CD37 expression and WHO grade (G), histology types (H), and IDH1 mutant status (I) in GSE16011.

(J–K) Correlations between CD37 expression and WHO grade (J) and histology types (K) in the Rembrandt cohort.

(L–M) Correlations between CD37 expression and WHO grade (L) and IDH1 mutant status (M) in the Xiangya cohort. ("NS" means no significance, *, **, ***mean p < 0.05, p < 0.01, p < 0.001, respectively.)

histopathology, and IDH or IDH1 mutation status, in diffuse gliomas from the TCGA cohort. We found that CD37 was highly expressed in gliomas with higher tumor grade (Figure 2A, p < 0.05) and GBM (Figure 2B, p < 0.05) than in other gliomas. In addition, CD37 was highly expressed in wild-type IDH gliomas compared with mutant IDH gliomas (Figure 2C, p < 0.05). Similar results were observed in the other three cohorts (p < 0.05, Figures 2D–2K), with higher CD37 expression in WHO IV glioma, wild-type IDH or IDH1 glioma, and GBM in the CGGA (Figures 2D–2F, p < 0.05), GSE16011 (Figures 2G–2I, p < 0.05) and Rembrandt cohorts (Figures 2J and 2K, p < 0.05). These results consistently demonstrated that the CD37 expression level was high in the malignant phenotype of diffuse gliomas. We further validated the CD37 expression pattern from our cohort containing 104 glioma samples and 27 normal brain tissues by qPCR. The results were highly consistent with those from the databases (Figure 2L, p < 0.05; Figure 2M, p < 0.05). To confirm the expression pattern of CD37, we performed immunohistochemistry (IHC) to evaluate the protein expression level of CD37 in the glioma tissue and found high-expression CD37 was enriched in higher grade and wild-type IDH1 gliomas (Figure S1). The above results demonstrated that diffuse gliomas with higher CD37 expression frequently exhibit a more aggressive malignant phenotype.

The prognostic significance of CD37 in diffuse gliomas

To explore the relationship between CD37 expression and the clinical outcome of diffuse glioma, we first performed univariate Cox regression analysis to examine the prognostic significance of CD37 across cancers. We observed that the expression of CD37 was significantly correlated with the OS of patients with eight types of cancers (Glioma, CESC, HNSC, LAML, LUAD, UCEC, UVM, and SKCM) (p < 0.05, Figure 3A). Specifically, Glioma, LAML, and UVM patients with high expression of CD37 had an unfavorable prognosis (HR > 1.0, p < 0.05) (Figure 3A), and CESC, HNSC, LUAD, SKCM, or UCEC patients with high CD37 expression had a favorable prognosis (HR < 1.0, p < 0.05) (Figure 3A). To analyze the impact of single tumor-related factors on the death of patients during the follow-up process, we further investigated the association of CD37 expression with DSS (disease-specific survival) in pan-cancer. High CD37 expression decreased DSS in Glioma and COAD patients (HR > 1.0, p < 0.05) and prolonged DSS in CESC, HNSC, KIRP, LUAD, SKCM, and UCEC patients (HR < 1.0, p < 0.05) (Figure 3B). Subsequently, we evaluated the relationship between CD37 expression and the progression-free interval (PFI) across cancers. Our findings
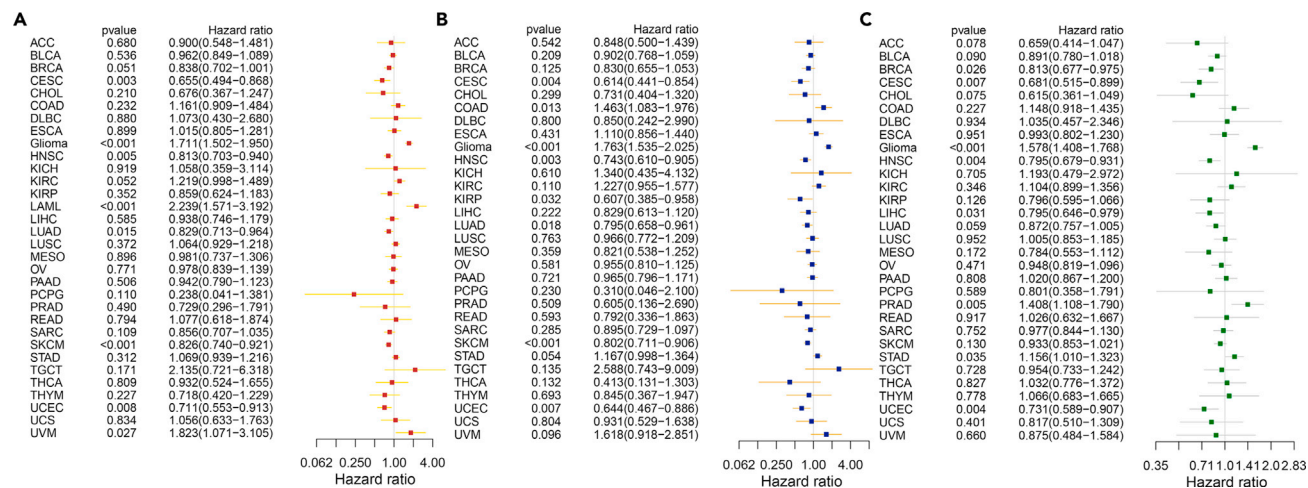
Figure 3. Correlations between CD37 expression with patients' clinical outcomes in pan-cancer.
(A–C) Forest plots showing the CD37 expression is related to patients' OS (A), DSS (B), and PFI (C) in pan-cancer. *P* < 0.05 was statistically different.

suggested that high expression of CD37 is an adverse factor for PFI in patients with Glioma, PRAD, or STAD (HR > 1.0, p < 0.05) and is a protective factor for PFI in BRCA, CESC, HNSC, LIHC, and UCEC patients (HR < 1.0, p < 0.05) (Figure 3C). The above results indicated that CD37 may be a vital underlying prognostic factor for gliomas.

Then, we performed Kaplan–Meier analysis to verify the association between CD37 expression and patients' survival time for diffuse gliomas in the TCGA, CGGA, GEO database: GSE16011, and Rembrandt cohorts. The Kaplan–Meier survival curves indicated that diffuse gliomas with high-expression CD37 displayed relatively unfavorable prognoses in the TCGA cohort (low expression: n = 280, median survival time = 79.9 months; high expression: n = 281, median survival time = 30.2 months, log-rank test p < 0.001, Figure 4A), which was validated in the other three cohorts (the CGGA cohort, low expression: n = 328, median survival time = 87.7 months; high expression: n = 328, median survival time = 20.1 months, log rank test p < 0.001; GSE16011, low expression: n = 128, median survival time = 20.3 months; high expression: n = 128, median survival time = 10.1 months, log rank test p < 0.001; the Rembrandt cohort, low expression: n = 196, median survival time = 27.2 months; high expression: n = 195, median survival time = 17.6 months, log rank test p < 0.001; Figures 4B–4D). The above results suggested that CD37 expression is associated with poor prognosis in diffuse gliomas.

Eventually, we estimated the independent predictive value of CD37 in glioma using univariate and multivariate Cox regression analyses. CD37 expression was associated with overall survival independent of other prognostic factors, including age, sex, grade, and mutation status of IDH or IDH1, in the four cohorts. In the CGGA cohort, we found that CD37 was an independent prognostic factor in the univariate Cox regression analysis (95% CI = 1.00–1.01, p < 0.05, Figure 4E) but not in the multivariate Cox regression analysis (p > 0.05, Figure 4F). Interestingly, patients with high CD37 expression often had a poor prognosis in the TCGA, Rembrandt, and GSE16011 cohorts (univariate Cox regression analysis: TCGA cohort, 95% CI = 1.05–1.10; GSE160121, 95% CI = 1.10–1.43; Rembrandt cohort, 95% CI = 1.05–1.47; multivariate Cox regression analysis: TCGA cohort, 95% CI = 1.02–1.07; GSE160121, 95% CI = 1.08–1.44; Rembrandt cohort, 95% CI = 1.01–1.45), independent of age, sex, grade, and mutation status of IDH or IDH1 (Figures 5G–5L, p < 0.05). Taken together, these results strongly confirmed that CD37 is an independent indicator of poor prognosis in patients with gliomas.

CD37 is related to immunologic pathways in diffuse gliomas

To investigate the biological process and underlying mechanisms of diffuse gliomas with different CD37 expression, we first divided all tumor samples into high-expression and low-expression groups based on the median value of CD37 expression in the TCGA, CGGA, GSE16011, and Rembrandt cohorts. By performing gene set enrichment analysis (GSEA), the results showed that CD37 was involved in biological
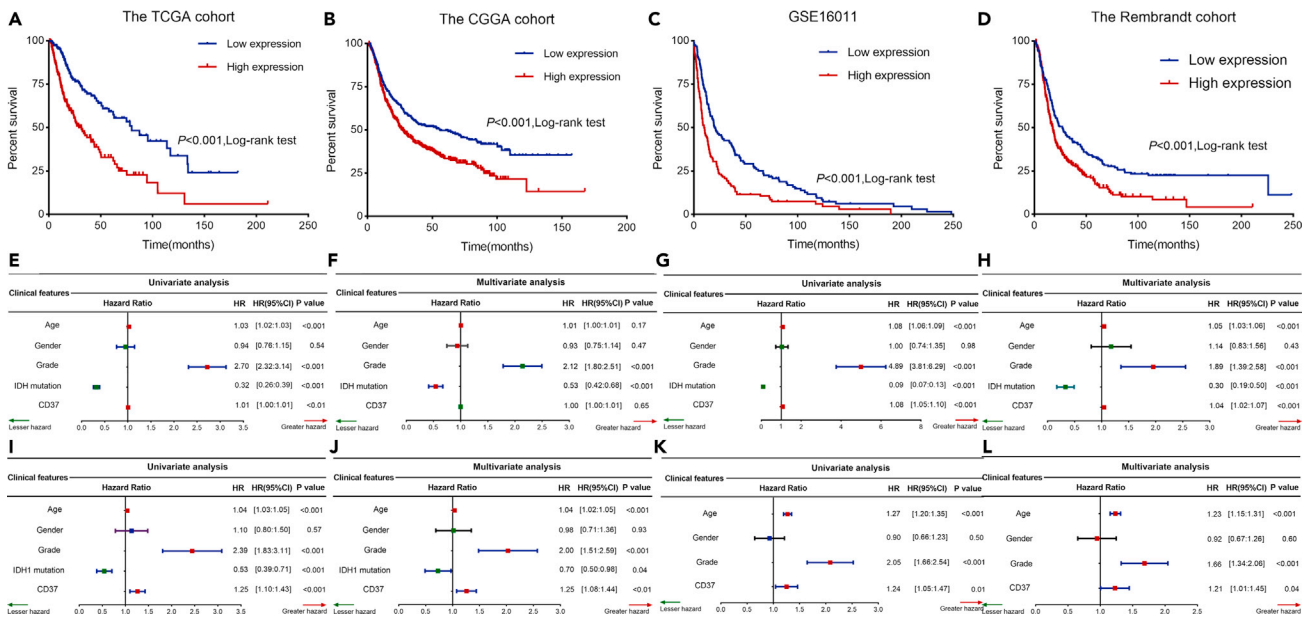
Figure 4. The prognostic value of CD37 expression for diffuse gliomas in the four cohorts

(A–D) Kaplan-Meier analysis of overall survival in the TCGA cohort (A), CGGA cohort (B), GSE16011 (C), and Rembrandt cohort (D) based on low- and high-expression of CD37. The red line represents samples with high-expression of CD37, and the blue line represents the samples with low-expression of CD37. p values were calculated by the log-rank test, and p < 0.05 was considered to be statistically different.

(E–F) Univariate (E) and multivariate (F) cox regression analysis in the CGGA cohort

(G and H) Univariate (G) and multivariate (H) cox regression analysis in the TCGA cohort

(I and J) Univariate (I) and multivariate (J) cox regression analysis in GSE16011

(K and L) Univariate (K) and multivariate (L) cox regression analysis in the Rembrandt cohort. CI, confidence interval; HR, hazard ratio; $P < 0.05$ was considered to be statistically different.

processes and underlying mechanisms, such as ''IL6/STAT3 signaling'', ''IL2/STAT5 signaling'', ''inflammatory response'', and ''NF-kappaB signaling''. Similar findings were observed in the four cohorts (Figures 5A–5D). To verify our results, we screened those genes that positively correlated with CD37 mRNA expression (Pearson r > 0.6, p < 0.001) by Pearson correlation analysis in the four cohorts (Table S1). Gene ontology (GO) enrichment analysis of CD37-associated genes indicated that CD37 plays an important role in regulating the immune response, including 'neutrophil activation', 'neutrophil degranulation, and 'neutrophil activation involved in immune response', in the TCGA, CGGA, GSE16011, and Rembrandt cohorts (Figures 5E–5H). These results indicated that CD37-related genes are mainly involved in immunologic pathways. Moreover, we also found that the pathways of CD37-associated genes were enriched in regulating the inflammatory response and STAT and NF-kappaB signaling pathways in the four cohorts (Table S2), which supported the above discoveries. In summary, our results showed that CD37 may be directly or indirectly correlated with immunologic biological processes in diffuse glioma.

The association between CD37 and immune infiltration in diffuse glioma

Considering that CD37 might be involved in immunologic biological processes in diffuse glioma, we assessed the relationship between the mRNA expression of CD37 and the immune and stromal scores by the ESTIMATE algorithm, which infers infiltrating stromal and immune cells. Pearson correlation analysis showed that CD37 was positively associated with immune and stromal scores in the TCGA cohort (immune score, r = 0.81; stromal score, r = 0.67) (p < 0.05, Figure 6A). The relationship between CD37 expression and immune and stromal scores was consistent with those in the CGGA (immune score, r = 0.74; stromal score, r = 0.57), GSE16011 (immune score, r = 0.83; stromal score, r = 0.63), and the Rembrandt cohorts (immune score, r = 0.86; stromal score, r = 0.68) (p < 0.05, Figures 6B–6D). In addition, we explored the relationship between CD37 expression and immune and stromal scores in 33 types of tumors, which suggested that CD37 expression was tightly associated with immune and stromal scores in most types of tumors (Figures S2 and S3). Thus, CD37 appears to be involved in modulating the constituents of the tumor microenvironment.
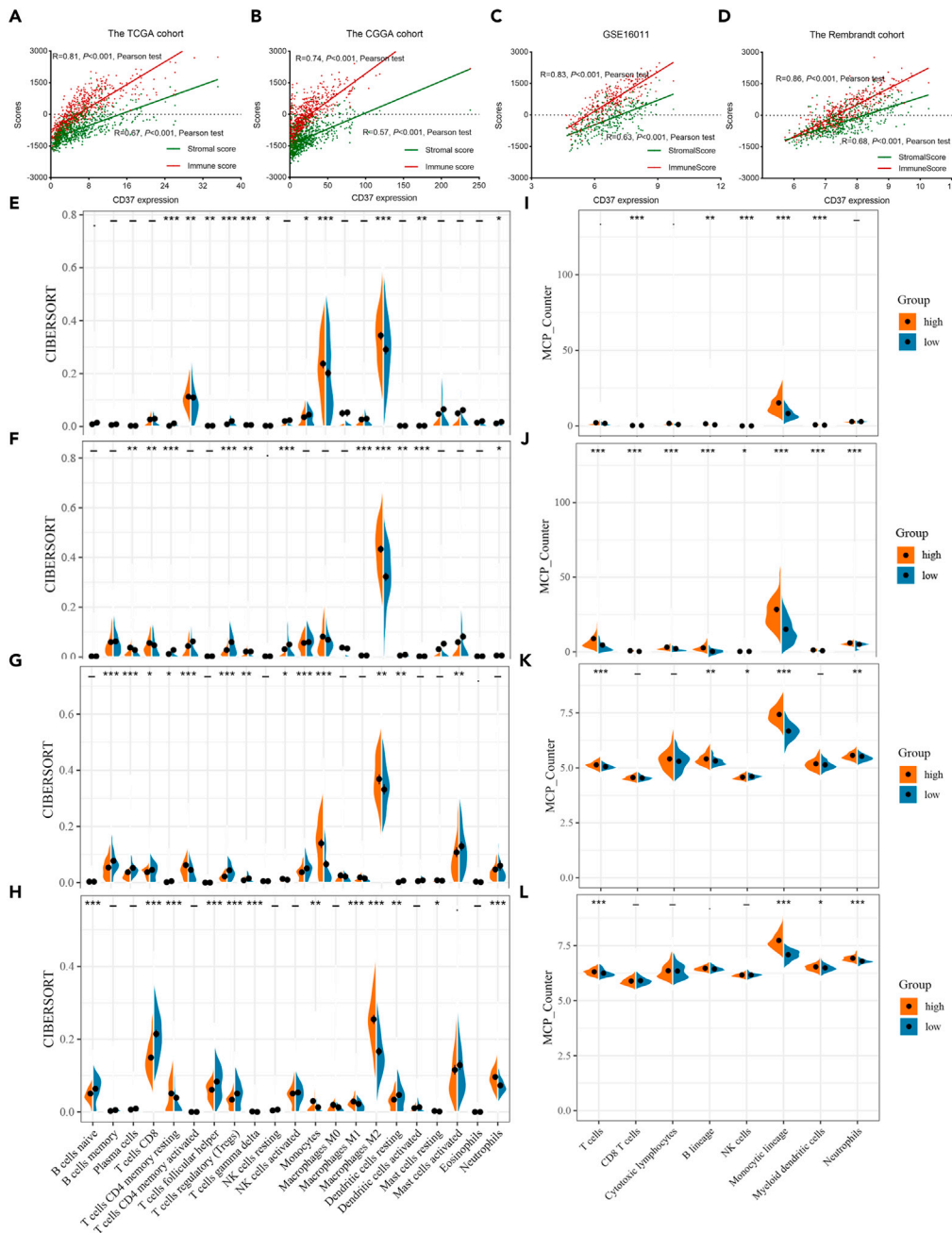
Figure 5. Functional enrichment analysis

(A–D) GSEA analysis of diffuse gliomas with low-expression and high-expression of CD37 in the TCGA cohort (A), CGGA cohort (B), GSE16011 (C), and Rembrandt cohort (D). The thresholds with a nominal p < 0.05 and an FDR <25% were considered as determining the significance of the enrichment score (ES)

(E–H) Gene ontology analysis for most associated-CD37 genes in the TCGA cohort (E), CGGA cohort (F), GSE16011 (G), and Rembrandt cohort (H).

We then used the CIBERSORT method to evaluate the relative abundance of 22 immune cell subtypes in diffuse gliomas and analyzed the difference in infiltrating immune cells between the high-expression and low-expression groups based on the median value of CD37 expression. A significant difference was observed between the two groups, with higher M2 abundance and lower follicular helper T cell abundances in the high-expression group than in the low-expression group in the TCGA cohort (Figure 6E, p < 0.05), which was validated in the other three cohorts (Figures 6F–6H, p < 0.05). We also found that diffuse gliomas with high CD37 expression exhibited a lower abundance of NK cells in the TCGA cohort and GSE16011 but no difference between those with high CD37 expression in the CGGA and Rembrandt cohorts compared with those with low CD37 expression (p < 0.05, Figures 6E–6H). Other immunosuppressive cells, including regulatory T cells (Tregs), M2 macrophages, mast cells, neutrophils, and monocytes, were enriched in diffuse gliomas with high CD37 expression in some of the four cohorts (p < 0.05, Figures 6E–6H). Therefore, we inferred that CD37 mediates immunosuppressive effects in the glioma microenvironment. However, contrary to our conclusion, a high abundance of neutrophils, a well-known immunosuppressive cell, was not enriched in diffuse gliomas with high CD37 expression in the TCGA cohort (p < 0.05, Figure 6E). We also performed the MCP-counter method to assess the absolute abundance of eight immune cell types. The results suggested diffuse gliomas with CD37 high expression had higher enriched monocytic lineage compared to the low expression group in the four cohorts, and the same results were observed for the abundance of neutrophils in other three cohorts except for the TCGA cohort (Figures 6I–6L, p < 0.05), which supports the idea that diffuse gliomas with high CD37 expression are characterized by immunosuppression. Anti-tumor CD8+ T cells were enriched in gliomas with high CD37 expression in the TCGA cohort (Figure 6I, p < 0.05), but no significant difference was observed in the other two cohorts (p > 0.05, Figure 6K and 6L). For the B lineage, diffuse gliomas with high CD37 expression had higher cell abundances as evaluated by the MCP-counter method in the TCGA, CGGA, and GSE16011 cohorts (Figures 6I–6K, p < 0.05) but not in the Rembrandt cohort (Figure 6L, p < 0.05). However, based on the Cibersort method, we did not find a significant difference between the two groups in the four cohorts (Figures 6E–6H, p < 0.05).

To investigate in which cell types CD37 was expressed, the single-cell data sequencing analysis was used, and the 18 cell clusters were identified in GEO database: GSE84465 (Darmanis et al., 2017) (Figures S4A and S4B). We also analyzed the distribution of CD37 and 10 molecular markers of B cells, CD8+ T cell, CD4+

Figure 6. Correlations of CD37 expression with immune and stromal infiltration level for diffuse gliomas

(A) The association between the mRNA expression of CD37 and immune and stromal scores in the TCGA cohort.

(B) The association between the mRNA expression of CD37 and immune and stromal scores in the CGGA cohort.

(C) The association between the mRNA expression of CD37 and immune and stromal scores in the GSE16011.

(D) The association between the mRNA expression of CD37 and immune and stromal scores in the Rembrandt cohort.

(E–H) The comparison of the cell abundance of 22 immune cells between gliomas with the low-expression and high-expression CD37 in the TCGA cohort (E), CGGA cohort (F), GSE16011 (G), and Rembrandt cohort (H).

(I–L) The comparison of abundance of eight types of immune cells between gliomas with low-expression and high-expression CD37 in the TCGA cohort (I), CGGA cohort (J), GSE16011 (K), and Rembrandt cohort (L). ("-" means no significance, *, **, *** mean p < 0.05, p < 0.01, p < 0.001, respectively.)

T cell, M1 macrophages, M2 macrophages, neutrophil, and dendritic cells in cell clusters, such as CD163, VSIG4, CD19, CD8A, CD8B, CD4, ITGAM, NRP1, ITGAX, NOS2, and the results uncovered CD37 and the markers of M2 macrophages, such as CD163 and VSIG4, shared a similar expression pattern (Figure S4C). In the glioma tissues, we also found gliomas with high-expression CD37 had up-regulated CD163 by IHC (Figure S4D). To further prove our observation, the expression of CD37 and CD163 in M2 macrophages induced by THP-1 was detected via qPCR assay (Figure S5), and the co-localization of CD37 and CD163 in M2 macrophages was detected by immunofluorescence assay (Figure S6). We observed the expression of CD37 in CD163-positive cells (M2), however, the expression of CD37 in CD163-negative cells (M0) induced by THP-1 was not found. These results indicated CD37 was expressed in the M2 macrophage of the glioma microenvironment. In a word, the results of immune infiltration analysis uncovered CD37 may play an important immunosuppressive role in diffuse glioma.

Correlation between CD37 and immune checkpoints

Accumulating literatures have reported that immune checkpoint therapy has provided new prospects against cancer (Postow et al., 2018; Zhao et al., 2019). To investigate whether CD37 can be used as a target for immune checkpoint therapy of glioma, we analyzed the correlation between CD37 expression and 37 checkpoint molecules and their corresponding ligands, such as CD80/CD86 for CTLA4 and PD-L1/PD-L2 for PD1, in diffuse glioma. Those results showed that CD37 was highly positively correlated with several immune checkpoint molecules, such as CD40 (TCGA, $r = 0.504$, CGGA, $r = 0.616$; GSE16011, $r = 0.248$; and Rembrandt, $r = 0.552$), CD48 (TCGA, $r = 0.546$, CGGA, $r = 0.724$; GSE16011, $r = 0.490$; and Rembrandt, $r = 0.574$), CD86 (TCGA, $r = 0.826$; CGGA, $r = 0.844$; GSE16011, $r = 0.829$; and Rembrandt, $r = 0.860$), HAVCR2(TCGA, $r = 0.861$; CGGA, $r = 0.806$; GSE16011, $r = 0.869$; and Rembrandt, $r = 0.824$), LAIR1(TCGA, $r = 0.824$; CGGA, $r = 0.723$; GSE16011, $r = 0.876$; and Rembrandt, $r = 0.856$), PD-L2 (TCGA, $r = 0.503$; CGGA, $r = 0.477$; GSE16011, $r = 0.331$; and Rembrandt, $r = 0.367$), and LGALS9 (TCGA, $r = 0.877$; CGGA, $r = 0.888$; GSE16011, $r = 0.852$; and Rembrandt, $r = 0.879$) (Pearson $r > 0.3$, $p < 0.05$, Table 1). In addition, CD37 expression had an intricate relationship with the mRNA expression of potentially targetable immune checkpoint genes, such as PD-L1 and PD-1, which are in clinical trials or have been approved for specific cancer types. We also found that CD37 expression had no significant correlation, or a weak correlation, with PD-L1 or PD-1 expression in the CGGA (PD-L1, $r = 0.270$, $p < 0.05$; PD-1, $r = 0.127$, $p < 0.05$), GSE16011 (PD-L1, $r = 0.082$, $p > 0.05$; PD-1, $r = -0.228$, $p < 0.05$), and Rembrandt cohorts (PD-L1, $r = 0.126$, $p < 0.05$; PD-1, $r = -0.032$, $p > 0.05$) (Pearson test, Table 1), whereas CD37 expression was weakly or moderately positively associated with PD-L1 or PD-1 expression, respectively, in the TCGA cohort (PD-L1, $r = 0.231$, $p < 0.05$; PD-1, $r = 0.400$, $p < 0.05$) (Pearson test, Table 1). These findings shed light on the crucial immunoregulatory role of CD37 in diffuse glioma, which suggests that targeting CD37 may provide a new path for immunotherapy of diffuse glioma.

DISCUSSION

Diffuse glioma is the most frequent intracranial primary tumor, and although the treatment has been improved, the mortality and recurrence rate of diffuse glioma remains high. Diffuse glioma is characterized by multistep and multigene redundant signaling pathways and an immunosuppressive microenvironment (Ma et al., 2018). In our study, we first analyzed the mRNA expression level of CD37 in normal tissues, indicating that the expression of CD37 was heterogeneous in different normal tissues and low in brain tissues (Figure 1A) ($p < 0.05$). In the pan-cancer analysis, CD37 was found to be abnormally expressed in most tumors (12/20) (Figure 1B), which was verified by combining the GTEX database and TCGA database (Figure 1C). In univariate Cox regression analysis, we also found that CD37 expression was significantly associated with patient OS, PFI, or DSS in multiple tumors, including glioma (Figure 3). These results showed that CD37 plays a critical role in tumors. The roles of CD37 in promoting tumorigenesis were reported in breast cancer (Kennedy and Harris, 2018) and B-cell malignancies (de Winde et al., 2016). Furthermore, accumulating literatures have revealed its selection as a target for therapy or prognostic indicators in multiple tumors (Leshchenko et al., 2010; Scarfò et al., 2018). Numerous studies have reported that CD37 plays a prominent role in the hematologic system (de Winde et al., 2016; Scarfò et al., 2018; Oostindie et al., 2020), which suggests that CD37 might be involved in regulating immune cells. By analyzing the TCGA, CGGA, GSE16011, and Rembrandt cohorts, we found that CD37 was highly expressed in high-grade diffuse gliomas, such as WHO IV glioma, wild-type IDH or IDH1 glioma, and GBM (Figures 2A–2K, $p < 0.05$), which was validated by qPCR in the Xiangya cohort (Figures 2L–2M, $p < 0.05$). Importantly, diffuse glioma patients with high CD37 expression exhibited poor clinical outcomes in the four cohorts (log-rank test $p < 0.001$, Figures 4A–4D). In the univariate and multivariate Cox regression analyses, CD37

Table 1. The correlations between CD37 expression and the mRNA expression of immune checkpoint genes in diffuse gliomas

Gene	TCGA r	TCGA p Value	CCGA r	CCGA p Value	GSE16011 r	GSE16011 p Value	Rembra ndt r	Rembra ndt p Value
BTLA	0.390	<0.001	0.357	<0.001	0.099	0.117	0.165	<0.001
CD160	0.067	0.084	0.010	0.011	−0.118	0.060	−0.129	0.007
CD200	−0.302	<0.001	−0.158	<0.001	−0.251	<0.001	−0.175	<0.001
CD200R1	0.396	<0.001	0.330	<0.001	0.105	0.094	0.036	0.445
CD244	0.384	<0.001	0.437	<0.001	0.005	0.932	−0.011	0.812
CD27	0.369	<0.001	0.463	<0.001	0.086	0.170	0.295	<0.001
CD274	0.231	<0.001	0.270	<0.001	0.082	0.193	0.126	0.008
CD276	0.263	<0.001	0.330	<0.001	0.344	<0.001	0.212	<0.001
CD28	0.352	<0.001	0.281	<0.001	0.100	0.111	0.192	<0.001
CD40	0.504	<0.001	0.616	<0.001	0.428	<0.001	0.552	<0.001
CD44	0.383	<0.001	0.249	<0.001	0.513	<0.001	0.403	<0.001
CD48	0.546	<0.001	0.724	<0.001	0.490	<0.001	0.574	<0.001
CD70	0.123	0.001	0.081	0.003	−0.111	0.076	0.058	0.226
CD80	0.467	<0.001	0.365	<0.001	0.196	0.002	0.239	<0.001
CD86	0.826	<0.001	0.844	<0.001	0.829	<0.001	0.860	<0.001
CTLA4	0.082	0.034	0.282	<0.001	−0.079	0.207	−0.043	0.365
HAVCR2	0.861	<0.001	0.806	<0.001	0.869	<0.001	0.824	<0.001
HHLA2	−0.025	0.519	0.064	0.091	−0.157	0.012	−0.210	<0.001
ICOS	0.426	<0.001	0.375	<0.001	0.085	0.176	0.144	0.002
ICOSLG	0.310	<0.001	0.540	<0.001	0.248	<0.001	0.429	<0.001
LAG3	0.254	<0.001	0.353	<0.001	−0.019	0.763	0.203	<0.001
LAIR1	0.824	<0.001	0.723	<0.001	0.876	<0.001	0.856	<0.001
LGALS9	0.877	<0.001	0.888	<0.001	0.852	<0.001	0.879	<0.001
NRP1	0.278	<0.001	0.138	<0.001	0.226	<0.001	0.183	<0.001
PDCD1	0.400	<0.001	0.127	<0.001	−0.228	<0.001	−0.032	0.495
PD-L2	0.503	<0.001	0.477	<0.001	0.331	<0.001	0.367	<0.001
TMIGD2	0.442	<0.001	0.363	<0.001	0.100	0.111	−0.111	0.020
TNFRSF18	0.140	<0.001	0.140	<0.001	−0.121	0.053	0.242	<0.001
TNFRSF25	0.195	<0.001	0.124	0.001	0.140	0.022	0.119	0.012
TNFRSF4	0.130	<0.001	0.197	<0.001	−0.146	0.020	0.080	0.093
TNFRSF8	0.219	<0.001	0.109	0.004	−0.118	0.061	0165	<0.001
TNFRSF9	0.226	<0.001	0.132	<0.001	−0.096	0.128	0.004	0.929
TNFSF14	0.407	<0.001	0.308	<0.001	0.209	<0.001	0.417	<0.001
TNFSF15	0.313	<0.001	0.194	<0.001	0.025	0.689	0.077	0.104
TNFSF18	0.076	0.050	0.088	0.021	−0.027	0.671	0.081	0.089
TNFSF9	0.042	0.278	0.157	<0.001	−0.107	0.088	−0.010	0.828
VTCN1	−0.100	0.010	0.017	0.662	−0.178	0.004	−0.074	0.119

r: Pearson correlation coefficient r.

proved to be a significantly unfavorable predictor for diffuse glioma patients, independent of age, sex, grade, and the mutation status of IDH or IDH1 (Figures 4E–4L, $p < 0.05$). However, the biological function of CD37 has not been reported in diffuse glioma. GSEA functional enrichment analysis of CD37 demonstrated immunologic processes, such as ''NF-κB signaling'', ''IL6/STAT3 signaling'', ''IL2/STAT5 signaling'', and ''inflammatory response'', were enriched in diffuse gliomas with high CD37 expression

(Figures 5A–5D). As an important addition, using GO enrichment analysis, we identified CD37-related genes were enriched in the pathways modulating the immune response, including "neutrophil activation", "neutrophil degranulation", and "neutrophil activation involved in immune response" (Figures 5E–5H). The subsequent immune cell infiltration analysis showed that macrophages, especially M2 macrophages, and neutrophils had a higher abundance in diffuse gliomas with high CD37 expression than in patients with low CD37 expression, while NK cells infiltrated to the opposite degree (Figure 6). Recent studies have revealed that diffuse gliomas with M2 macrophage and neutrophil infiltration have a poor prognosis (Zhang et al., 2017; Wei et al., 2019), which is consistent with our findings, suggesting that CD37 may affect malignant progression by regulating the infiltration of M2 macrophages and neutrophils in diffuse gliomas.

Previous research has shown that activated neutrophils and macrophages can produce tumor necrosis factor (TNF) and induce proinflammatory cytokines, such as IL-1, to promote tumorigenesis (Balkwill, 2009). It has also been reported that IL-1 can activate the NF-κB pathway and promote the progression of colon cancer (Voronov and Apte, 2015). In addition, the literature has reported that the differentiation of tumor-associated macrophages into M2 macrophages and the lytic function of NK cells are mediated through the NF-kB signaling pathway (Hagemann et al., 2008). These results support our findings that CD37 remodels the immunosuppressive microenvironment of gliomas through the NF-kB signaling pathway to evade immune surveillance and promote malignant progression in diffuse gliomas.

CD37 plays a vital immunosuppressive role in glioma, and its high expression indicates a poor prognosis, which may also be attributable to the IL-6/STAT3 signaling pathway. IL-6 produced by macrophages is a well-researched protumorigenic cytokine, and its expression level is often related to the poor prognosis of tumors (Taniguchi and Karin, 2014). Therefore, we inferred that CD37 may activate the NF-κB pathway by recruiting more neutrophils, thus inhibiting the cytolytic activity of NK cells and CD8^{+} T cells, promoting the polarization of M2 macrophages, and promoting the malignant progression of gliomas. These results partly explain how CD37 exerts its immunosuppressive effect to promote tumor progression in diffuse glioma.

The literature indicates that CD37 is widely located on the B-cell surface but not resting T cells, natural killer cells, or macrophages (Schwartz-Albiez et al., 1988) and is involved in regulating immunity and suppressing tumors (Xu-Monette et al., 2016). Some literatures have reported that the absence of CD37 drives tumor development through activation of the IL-6 signaling pathway (de Winde et al., 2016), which contradicts our results that CD37 serves as a tumor promoter. However, our research showed that the association between CD37 and the abundance of B lineage cells was not consistently validated in the four cohorts (Figure 6), which does not fully explain the results reported in the literature. Thus, we inferred that CD37 is also expressed by other types of cells, including glioma cells, and its abnormal expression might recruit more immunosuppressive cells, such as regulatory T cells (Tregs), M2 macrophages, mast cells, and neutrophils, and impair the normal function of B cells. These hypotheses and contradictions need to be further verified experimentally.

In recent years, checkpoint-targeted immunotherapy has achieved remarkable success in some tumors (Hodi et al., 2018; Rizvi et al., 2015), including diffuse glioma (Lim et al., 2018). In our study, CD37 was tightly associated with some of the checkpoint molecules, such as CD276, CD48, CD40, LGALS9, LAIR1, CD86, PD-L2, and HAVCR2, in the four cohorts (Table 1, Pearson test, $p < 0.05$), indicating that blocking CD37 might enhance the efficacy of checkpoint inhibition.

Limitations of the study

This research mainly uncovered CD37 plays a role of immunosuppression in diffuse glioma microenvironment, while how CD37 operates to induce immune cells suppression is unclear, which could be considered to extend the present study in the future.

STAR★METHODS

Detailed methods are provided in the online version of this paper and include the following:

- KEY RESOURCES TABLE
- RESOURCE AVAILABILITY
  - Lead contact
  - Materials availability

SUPPLEMENTAL INFORMATION

Supplemental information can be found online at https://doi.org/10.1016/j.isci.2021.103249.

ABBREVIATIONS

ACC   adrenocortical carcinoma

BLCA   bladder urothelial carcinoma

BRCA   breast invasive carcinoma

CESC   cervical squamous cell carcinoma

CGGA   Chinese Glioma Genome Atlas

CHOL   cholangiocarcinoma

COAD   colon adenocarcinoma

DLBC   lymphoid neoplasm diffuse large B cell lymphoma

ESCA   esophageal carcinoma

GBM   glioblastoma multiforme

GO   gene ontology

GSEA   gene set enrichment analysis

GTEx   the Genotype-Tissue Expression

HNSC   head and neck squamous cell carcinoma

IDH1   isocitrate dehydrogenase 1

KICH   kidney chromophobe

KIRC   kidney renal clear cell carcinoma

KIRP   kidney renal papillary cell carcinoma

LAML   acute myeloid leukemia

LGG   brain lower grade glioma

LIHC   liver hepatocellular carcinoma

LUAD   lung adenocarcinoma

LUSC   lung squamous cell carcinoma

MESO   mesothelioma

OV	ovarian serous cystadenocarcinoma
PAAD	pancreatic adenocarcinoma
PCPG	pheochromocytoma and paraganglioma
PRAD	prostate adenocarcinoma
qPCR	quantitative real-time polymerase chain reaction
READ	rectum adenocarcinoma
SARC	sarcoma
SKCM	skin cutaneous melanoma
STAD	stomach adenocarcinoma
TCGA	The Cancer Genome Atlas
TGCT	testicular germ cell tumors
THCA	thyroid carcinoma
THYM	thymoma
TNF	tumor necrosis factor
UCEC	uterine corpus endometrial carcinoma
UCS	uterine carcinosarcoma
UVM	uveal melanoma

AUTHOR CONTRIBUTIONS

Q.W.Z, C.P. R, and X.J.J conceived and designed the study, X.J.Y and Q.W.Z analyzed the results. Other authors performed analysis procedures. Q.W.Z and X.J.Y wrote the manuscript, X.J.Y revised the manuscript. All authors contributed to the editing of the manuscript.

DECLARATION OF INTERESTS

The authors declare no competing interests.

REFERENCES

Balkwill, F. (2009). Tumour necrosis factor and cancer. Nat. Rev. Cancer 9, 361–371.

Becht, E., Giraldo, N.A., Lacroix, L., Buttard, B., Elarouci, N., Petitprez, F., Selves, J., Laurent-Puig, P., Sautès-Fridman, C., Fridman, W.H., et al. (2016). Estimating the population abundance of tissue-infiltrating immune and stromal cell populations using gene expression. Genome Biol. 17, 218.

Cancer Genome Atlas Research Network, Brat, D.J., Verhaak, R.G., Aldape, K.D., Yung, W.K., Salama, S.R., Cooper, L.A., Rheinbay, E., Miller, C.R., Vitucci, M., et al. (2015). Comprehensive, integrative genomic analysis of diffuse lower-grade gliomas. N. Engl. J. Med. 72, 2481–2498.

Cooper, M.L., Choi, J., Staser, K., Ritchey, J.K., Devenport, J.M., Eckardt, K., Rettig, M.P., Wang, B., Eissenberg, L.G., Ghobadi, A.,

et al. (2018). An ''off-the-shelf'' fratricide-resistant CAR-T for the treatment of T cell hematologic malignancies. Leukemia 32, 1970–1983.

Darmanis, S., Sloan, S.A., Croote, D., Mignardi, M., Chernikova, S., Samghababi, P., Zhang, Y., Neff, N., Kowarsky, M., Caneda, C., et al. (2017). Single-cell RNA-seq analysis of infiltrating neoplastic cells at the migrating front of human glioblastoma. Cell Rep 21, 1399–1410.

Friebel, E., Kapolou, K., Unger, S., Núñez, N.G., Utz, S., Rushing, E.J., Regli, L., Weller, M., Greter, M., Tugues, S., et al. (2020). Single-cell mapping of human brain cancer reveals tumor-specific instruction of tissue-invading leukocytes. Cell 181, 1626–1642.

Graeber, M.B., Scheithauer, B.W., and Kreutzberg, G.W. (2002). Microglia in brain tumors. Glia 40, 252–259.

Hagemann, T., Lawrence, T., McNeish, I., Charles, K.A., and Kulbe, H. (2008). Thompson RG, Robinson SC, Balkwill FR. "Re-educating" tumor-associated macrophages by targeting NF-kappaB. J. Exp. Med. 205, 1261–1268.

Hodi, F.S., Chiarion-Sileni, V., Gonzalez, R., Grob, J.J., Rutkowski, P., Cowey, C.L., Lao, C.D., Schadendorf, D., Wagstaff, J., Dummer, R., et al. (2018). Nivolumab plus ipilimumab or nivolumab alone versus ipilimumab alone in advanced melanoma (CheckMate 067): 4-year outcomes of a multicentre, randomised, phase 3 trial. Lancet Oncol. 19, 1480–1492.

Hussain, S.F., Yang, D., Suki, D., Aldape, K., Grimm, E., and Heimberger, A.B. (2006). The role of human glioma-infiltrating microglia/macrophages in mediating antitumor immune responses. Neuro Oncol. 8, 261–279.

Kennedy, B.M., and Harris, R.E. (2018). Cyclooxygenase and lipoxygenase gene expression in the inflammogenesis of breast cancer. Inflammopharmacology 26, 909–923.

Leshchenko, V.V., Kuo, P.Y., Shaknovich, R., Yang, D.T., Gellen, T., Petrich, A., Yu, Y., Remache, Y., Weniger, M.A., Rafiq, S., et al. (2010). Genomewide DNA methylation analysis reveals novel targets for drug development in mantle cell lymphoma. Blood 116, 1025–1034.

Liang, J., Piao, Y., Holmes, L., Fuller, G.N., Henry, V., Tiao, N., and de Groot, J.F. (2014). Neutrophils promote the malignant glioma phenotype through S100A4. Clin. Cancer Res. 20, 187–198.

Lim, M., Xia, Y., Bettegowda, C., and Weller, M. (2018). Current state of immunotherapy for glioblastoma. Nat. Rev. Clin. Oncol. 15, 422–442.

Liu, J., Huang, W., Ren, C., Wen, Q., Liu, W., Yang, X., Wang, L., Zhu, B., Zeng, L., Feng, X., et al. (2015). Flotillin-2 promotes metastasis of nasopharyngeal carcinoma by activating NF-κB and PI3K/Akt3 signaling pathways. Sci. Rep. 24, 11614.

Louis, D.N., Perry, A., Reifenberger, G., von Deimling, A., Figarella-Branger, D., Cavenee, W.K., Ohgaki, H., Wiestler, O.D., Kleihues, P., and Ellison, D.W. (2016). The 2016 World Health Organization classification of tumors of the central nervous system: a summary. Acta Neuropathol. 131, 803–820.

Ma, Q., Long, W., Xing, C., Chu, J., Luo, M., Wang, H.Y., Liu, Q., and Wang, R.F. (2018). Cancer stem cells and immunosuppressive microenvironment in glioma. Front Immunol. 9, 2924.

Martínez-Ricarte, F., Mayor, R., Martínez-Sáez, E., Rubio-Pérez, C., Pineda, E., Cordero, E., Cicuéndez, M., Poca, M.A., López-Bigas, N., Ramon, Y., Cajal, S., et al. (2018). Molecular diagnosis of diffuse gliomas through sequencing of cell-free circulating tumor DNA from cerebrospinal fluid. Clin. Cancer Res. 24, 2812–2819.

Meyer-Wentrup, F., Figdor, C.G., Ansems, M., Brossart, P., Wright, M.D., Adema, G.J., and van Spriel, A.B. (2007). Dectin-1 interaction with tetraspanin CD37 inhibits IL-6 production. J. Immunol. 178, 154–162.

Mounir, M., Lucchetta, M., Silva, T., C, Olsen, C., Bontempi, G., Chen, X., Noushmehr, H., Colaprico, A., and Papaleo, E. (2019). New functionalities in the TCGAbiolinks package for the study and integration of cancer data from GDC and GTEx. PLoS Comput Biol. 15, e1006701.

Murray, P.J., Allen, J.E., Biswas, S.K., Fisher, E.A., Gilroy, D.W., Goerdt, S., Gordon, S., Hamilton, J.A., Ivashkiv, L.B., Lawrence, T., et al. (2014). Macrophage activation and polarization: nomenclature and experimental guidelines. Immunity 41, 14–20.

Newman, A.M., Liu, C.L., Green, M.R., Gentles, A.J., Feng, W., Xu, Y., Hoang, C.D., Diehn, M., and Alizadeh, A.A. (2015). Robust enumeration of cell subsets from tissue expression profiles. Nat. Methods 12, 453–457.

Oostindie, S.C., van der Horst, H.J., Kil, L.P., Strumane, K., Overdijk, M.B., van den Brink, E.N., van den Brakel, J.H.N., Rademaker, H.J., et al. (2020). DuoHexaBody-CD37®, a novel biparatopic CD37 antibody with enhanced Fc-mediated hexamerization as a potential therapy for B-cell malignancies. Blood Cancer J. 10, 30.

Ostrom, Q.T., Gittleman, H., Xu, J., Kromer, C., Wolinsky, Y., Kruchko, C., and Barnholtz-Sloan, J.S. (2016). CBTRUS statistical report: primary brain and other central nervous system tumors diagnosed in the United States in 2009-2013. Neuro Oncol. 1, v1–v75.

Pagel, J.M., Spurgeon, S.E., Byrd, J.C., Awan, F.T., Flinn, I.W., Lanasa, M.C., Eisenfeld, A.J., Stromatt, S.C., and Gopal, A.K. (2015). Otlertuzumab (TRU-016), an anti-CD37 monospecific ADAPTIR(™) therapeutic protein, for relapsed or refractory NHL patients. Br. J. Haematol. 168, 38–45.

Pereira, D.S., Guevara, C.I., Jin, L., Mbong, N., Verlinsky, A., Hsu, S.J., Aviña, H., Karki, S., Abad, J.D., Yang, P., et al. (2015). AGS67E, an anti-CD37 monomethyl auristatin E antibody-drug conjugate as a potential therapeutic for B/T-Cell malignancies and AML: a new role for CD37 in AML. Mol. Cancer Ther. 14, 1650–1660.

Perry, J.R., Laperriere, N., O'Callaghan, C.J., Brandes, A.A., Menten, J., Phillips, C., Fay, M., Nishikawa, R., Cairncross, J.G., Roa, W., et al. (2017). Trial investigators. Short-course radiation plus temozolomide in elderly patients with glioblastoma. N. Engl. J. Med. 16, 1027–1037.

Postow, M.A., Sidlow, R., and Hellmann, M.D. (2018). Immune-related adverse events associated with immune checkpoint blockade. N. Engl. J. Med. 378, 158–168.

Quail, D.F., and Joyce, J.A. (2017). The microenvironmental landscape of brain tumors. Cancer Cell 31, 326–341.

Reardon, D.A., Freeman, G., Wu, C., Chiocca, E.A., Wucherpfennig, K.W., Wen, P.Y., Fritsch, E.F., Curry, W.T., Jr., Sampson, J.H., and Dranoff, G. (2014). Immunotherapy advances for glioblastoma. Neuro Oncol. 16, 1441–1458.

Rizvi, N.A., Mazières, J., Planchard, D., Stinchcombe, T.E., Dy, G.K., Antonia, S.J., Horn, L., Lena, H., Minenza, E., Mennecier, B., et al. (2015). Activity and safety of nivolumab, an anti-PD-1 immune checkpoint inhibitor, for patients with advanced, refractory squamous non-small-cell lung cancer (CheckMate 063): a phase 2, single-arm trial. Lancet Oncol. 16, 257–265.

Scarfò, I., Ormhøj, M., Frigault, M.J., Castano, A.P., Lorrey, S., Bouffard, A.A., van Scoyk, A., Rodig, S.J., Shay, A.J., Aster, J.C., et al. (2018). Anti-CD37 chimeric antigen receptor T cells are active against B- and T-cell lymphomas. Blood 132, 1495–1506.

Schwartz-Albiez, R., Dörken, B., Hofmann, W., and Moldenhauer, G. (1988). The B cell-associated CD37 antigen (gp40-52). Structure and subcellular expression of an extensively glycosylated glycoprotein. J. Immunol. 140, 905–914.

Schwartzbaum, J.A., Fisher, J.L., Aldape, K.D., and Wrensch, M. (2006). Epidemiology and molecular pathology of glioma. Nat. Clin. Pract. Neurol. 2, 494–503.

van Spriel, A.B., Puls, K.L., Sofi, M., Pouniotis, D., Hochrein, H., Orinska, Z., Knobeloch, K.P., Plebanski, M., and Wright, M.D. (2004). A regulatory role for CD37 in T cell proliferation. J. Immunol. 172, 2953–2961.

Stupp, R., Hegi, M.E., Mason, W.P., van, den, Bent, M.J., Taphoorn, M.J., Janzer, R.C., Ludwin, S.K., Allgeier, A., Fisher, B., et al. (2009). Effects of radiotherapy with concomitant and adjuvant temozolomide versus radiotherapy alone on survival in glioblastoma in a randomised phase III study: 5-year analysis of the EORTC-NCIC trial. Lancet Oncol. 10, 459–466.

Subramanian, A., Tamayo, P., Mootha, V.K., Mukherjee, S., Ebert, B.L., Gillette, M.A., Paulovich, A., Pomeroy, S.L., Golub, T.R., Lander, E.S., et al. (2005). Gene set enrichment analysis: a knowledge-based approach for interpreting genome-wide expression profiles. Proc. Natl. Acad. Sci. U S A 102, 15545–51550.

Suzuki, H., Aoki, K., Chiba, K., Sato, Y., Shiozawa, Y., Shiraishi, Y., Shimamura, T., Niida, A., Motomura, K., Ohka, F., et al. (2015). Mutational landscape and clonal architecture in grade II and III gliomas. Nat. Genet. 47, 458–468.

Taniguchi, K., and Karin, M. (2014). IL-6 and related cytokines as the critical lynchpins between inflammation and cancer. Semin. Immunol. 26, 54–74.

Voronov, E., and Apte, R.N. (2015). IL-1 in colon inflammation, colon carcinogenesis and invasiveness of colon cancer. Cancer Microenviron 8, 187–200.

Wee, J.L., Schulze, K.E., Jones, E.L., Yeung, L., Cheng, Q., Pereira, C.F., Costin, A., Ramm, G.,

van Spriel, A.B., Hickey, M.J., et al. (2015). Tetraspanin CD37 regulates β2 integrin-mediated adhesion and migration in neutrophils. J. Immunol. *195*, 5770–5779.

Wei, J., Marisetty, A., Schrand, B., Gabrusiewicz, K., Hashimoto, Y., Ott, M., Grami, Z., Kong, L.Y., Ling, X., Caruso, H., et al. (2019). Osteopontin mediates glioblastoma-associated macrophage infiltration and is a potential therapeutic target. J. Clin. Invest *129*, 137–149.

de Winde, C.M., Veenbergen, S., Young, K.H., Xu-Monette, Z.Y., Wang, X.X., Xia, Y., Jabbar, K.J., van den, Brand, M., van der, et al.. (2016). Tetraspanin CD37 protects against the development of B cell lymphoma. J. Clin. Invest *126*, 653–666.

Xu-Monette, Z.Y., Li, L., Byrd, J.C., Jabbar, K.J., Manyam, G.C., Maria de, Winde.C., van den,

Brand.M., Tzankov, A., Visco, C., Wang, J., et al. (2016). Assessment of CD37 B-cell antigen and cell of origin significantly improves risk prediction in diffuse large B-cell lymphoma. Blood *128*, 3083–3100.

Yi, M., Jiao, D., Xu, H., Liu, Q., Zhao, W., Han, X., and Wu, K. (2018). Biomarkers for predicting efficacy of PD-1/PD-L1 inhibitors. Mol. Cancer *17*, 129.

Yoshihara, K., Shahmoradgoli, M., Martínez, E., Vegesna, R., Kim, H., Torres-Garcia, W., Treviño, V., Shen, H., Laird, P.W., Levine, D.A., et al. (2013). Inferring tumour purity and stromal and immune cell admixture from expression data. Nat. Commun. *4*, 2612.

Yu, G., Wang, L.G., Han, Y., and He, Q.Y. (2012). clusterProfiler: an R package for comparing

biological themes among gene clusters. OMICS *16*, 284–287.

Zhang, C., Cheng, W., Ren, X., Wang, Z., Liu, X., Li, G., Han, S., Jiang, T., and Wu, A. (2017). Tumor purity as an underlying key factor in glioma. Clin. Cancer Res. *23*, 6279–6291.

Zhao, J., Chen, A.X., Gartrell, R.D., Silverman, A.M., Aparicio, L., Chu, T., Bordbar, D., Shan, D., Samanamud, J., Mahajan, A., et al. (2019). Immune and genomic correlates of response to anti-PD-1 immunotherapy in glioblastoma. Nat. Med. *25*, 462–469.

Zhou, Q., Yan, X., Liu, W., Yin, W., Xu, H., Cheng, D., Jiang, X., and Ren, C. (2020). Three immune-associated subtypes of diffuse glioma differ in immune infiltration, immune checkpoint molecules, and prognosis. Front Oncol. *10*, 586019.

STAR★METHODS

KEY RESOURCES TABLE

REAGENT or RESOURCE	SOURCE	IDENTIFIER
Antibodies		
Rabbit polyclonal anti-CD37	Proteintech	RRID:21044–1-AP
Mouse monoclonal anti-CD163	AiFang biological	RRID:AF20010
Chemicals, peptides, and recombinant proteins		
Phorbol 12-myristate 13-acetate (PMA)	MedChemExpress	Cat#HY-18739
Recombinant Human Interleukin-4	Sangon Biotech	Cat#C610006
Recombinant Human Interleukin-13	Sangon Biotech	Cat#C620012
Critical commercial assays		
SYBR qPCR Master Mix	Vazyme	Vazyme Code: Cat#Q711-02
RNA with a reverse transcription kit	Thermo Fisher Scientific	Cat#K1622
Deposited data		
The mRNA expression of CD37 for 33 types of tumors and 30 types of normal tissues	UCSC Xena platform	https://xena.ucsc.edu/
The clinical data of glioma patients and their corresponding gene expression profiles	The Chinese Glioma Genome Atlas	http://www.cgga.org.cn
GSE16011 database	Gene Expression Omnibus	https://www.ncbi.nlm.nih.gov/geo/query/acc.cgi?acc=GSE16011
The Rembrandt database	Gene Expression Omnibus	https://www.ncbi.nlm.nih.gov/geo
Experimental models: cell lines		
THP-1	Laboratory of Yizhou Zou	N/A
Oligonucleotides		
CD37 forward primer: 5′- AGCTGGGACTATGTGCAGTTCC-3′	This paper	N/A
CD37 reverse primer: 5′- CCGACAAGTTGTAGCAGGAGCA-3′	This paper	N/A
ACTB forward primer: 5′-ACAGAGCCTCGCCTTTGCGGAT-3′	This paper	N/A
ACTB reverse primer: 5′- CTTGCACATGCCGGAGCCGTT -3′	This paper	N/A
CD163 forward primer: 5′-CCAGAAGGAACTTGTAGCCACAG-3′	This paper	N/A
CD163 reverse primer: 5′-CAGGCACCAAGCGTTTTGAGCT-3′	This paper	N/A
NOS2 forward primer: 5′-GCTCTACACCTCCAATGTGACC-3′	This paper	N/A
NOS2 reverse primer: 5′-CTGCCGAGATTTGAGCCTCATG-3′	This paper	N/A
Software and algorithms		
R (vision 4.0.5)	Downloaded from the R Project for Statistical Computing	https://www.r-project.org/
GSEA software (vision 3.0)	Downloaded from the Broad Institute	http://www.broadinstitute.org/gsea

RESOURCE AVAILABILITY

Lead contact

Further information could be directly consulted to the lead contact, Caiping Ren (rencaiping@csu.edu.cn).

Materials availability

This research did not generate new materials.

Data and code availability

This paper analyzes existing publicly available data and those datasets are listed in the key resources table. This paper does not report original code. Any other additional information required to reanalyze the data reported in this paper is available from the lead contact upon request.

EXPERIMENTAL MODEL AND SUBJECT DETAILS

Cell lines

THP-1 cells were donated by Dr. Huiyun Peng of Lab Yizhou Zou which was incubated in RPMI 1640 supplemented with 10% FBS at 37°C with 5% CO_2.

METHOD DETAILS

Data source and data processing

We downloaded data on the mRNA expression of CD37 for 33 types of tumors and 30 types of normal tissues from the UCSC Xena platform (https://xena.ucsc.edu/), which assembled the Cancer Genome Atlas (TCGA) database and the Genotype-Tissue Expression (GTEx) database. The mRNA expression data of TCGA and GTEx were combined into one dataset after undergone the same normalization by using the TCGAbiolinks package (Mounir et al., 2019). The clinical data of patients and their corresponding gene expression profiles were downloaded from public datasets of the TCGA dataset, the Chinese Glioma Genome Atlas (CGGA) dataset (n = 693) (http://www.cgga.org.cn) (n = 703), the GSE16011 database (n = 276), and the Rembrandt database (n = 471) (https://www.ncbi.nlm.nih.gov/geo). Duplicate samples in TCGA were removed, and 677 samples that met the criteria were screened.

Patients of the Xiangya cohort

This study was approved by the Ethics Committee of Xiangya Hospital, Central South University. The clinical samples of gliomas (n = 104) were all collected from Xiangya Hospital, Central South University. Written informed consent was obtained from all patients.

Quantitative real-time polymerase chain reaction (qPCR)

According to the protocol provided by the manufacturer, total RNA from fresh tissue was extracted using TRIzol (Life Technologies). Complementary DNA was synthesized from total RNA with a reverse transcription kit (Thermo Fisher Scientific). Real-time qPCR was executed with SYBR qPCR Master Mix (Vazyme). ACTB was used as an internal reference gene, and $2^{-\Delta\Delta Ct}$ was used to quantify the relative expression level of CD37. The primer sequences were listed in the Key Resources Table.

Survival analysis

We first removed samples with overall survival of fewer than 30 days and missing clinical characteristic data. The relationship between the expression level of CD37 mRNA and the overall survival (OS), disease-specific survival (DSS), and progression-free interval (PFI) of tumor patients is displayed in forest plots. In addition, the Kaplan–Meier method was used to estimate patient OS for diffuse glioma in the four cohorts. Finally, univariate Cox and multivariate Cox regression models were used to assessing the independent predictive value of clinical and pathological features, including age, sex, grade, CD37 expression, and IDH status or IDH1. $p < 0.05$ indicates that the difference is statistically significant.

Functional enrichment analysis of CD37

The underlying signaling pathways of CD37 were explored via gene set enrichment analysis (GSEA) using GSEA software (vision 3.0) that was downloaded from the Broad Institute (http://www.broadinstitute.org/gsea) (Subramanian et al., 2005). According to the median value of CD37 expression, all samples were

divided into high and low expression groups. The two sets of gene expression profiles in the four cohorts and hallmark gene sets from the MSigDB dataset were imported into GSEA software, and the normalized enrichment scores and p values of each biological pathway were obtained by GSEA. According to Pearson correlation analysis, we selected the genes that were most related to CD37 with a correlation co-efficient r > 0.6 (p < 0.001). The Gene Ontology categories of CD37-related genes were performed by a cluster profile package (Yu et al., 2012). The threshold was defined as p < 0.05.

Estimation of immune and stromal infiltration

According to the gene expression profile, the ESTIMATE package was used to assess immune and stromal scores, which can evaluate the abundance of immune cells and stromal cells (Yoshihara et al., 2013). In addition, we performed the CIBERSORT method to assess the relative levels of 22 types of immune cells (Newman et al., 2015). In addition, the absolute abundance of eight types of immune cells was assessed by MCP-counter (Becht et al., 2016).

Immunohistochemistry and immunofluorescence

Immunohistochemical detection of CD37 and CD163 was performed according to a previously described method (Liu et al., 2015). In brief, antibodies against CD37 and CD163 were incubated overnight at 4°C, and a secondary antibody was then incubated at room temperature for 60 min. The primary antibodies used in this study included anti-CD37 (21044–1-AP, 1:50) and anti-CD163 (AF20010, 1:50).

THP-1 cells were seeded into 6-well plates and cultured in RPMI 1640 supplemented with 10% FBS. Then, THP-1 cells were differentiated into M0 macrophages via phorbol 12-myristate 13-acetate (PMA) (200 nmol/L) for 2 days, and the M0 cells were further polarized into M2 macrophages under the stimulus of IL-13 and IL-4 (20 ng/mL). M0 and M2 macrophages were seeded into 6-well plates and cultured in RPMI 1640 supplemented with 10% FBS. The cells were washed with PBS three times and incubated with 4% para-formaldehyde for 30 min at room temperature. Then, the cells were washed with PBS again and blocked for 30 min in bovine serum albumin, followed by incubation with anti-CD163/anti-CD37 (CD37 1:50, CD163 1:50) primary antibody overnight at 4°C. After that, the cells were incubated with the corresponding fluo-rescently labeled secondary antibody for 60 min at room temperature. Finally, the cell nuclei were stained with DAPI for 1 minute. Immunofluorescence microscopy was used to monitor cellular fluorescence.

QUANTIFICATION AND STATISTICAL ANALYSIS

The unpaired t test was used to evaluate the expression of CD37 in the normal group and tumor groups and the IDH or IDH1 mutant group and wild-type groups. The Kruskal–Wallis test was used to compare nonparametric differences between different histological subtypes. Pearson correlation analysis was used to examine the correlation between CD37 expression and 38 immune checkpoint molecules, immune scores, and stromal scores. All statistical data were analyzed using GraphPad Prism 7.0 or R soft-ware (www.r-project.org). p < 0.05 was defined as statistically significant, and *, **, *** indicate p < 0.05, p < 0.01, and p < 0.001, respectively.